

Accelerated Article Preview

Age-specific mortality and immunity patterns of SARS-CoV-2

Received: 24 August 2020

Accepted: 23 October 2020

Accelerated Article Preview Published
online 2 November 2020

Cite this article as: O'Driscoll, M. et al.
Age-specific mortality and immunity
patterns of SARS-CoV-2. *Nature*
<https://doi.org/10.1038/s41586-020-2918-0>
(2020).

Megan O'Driscoll, Gabriel Ribeiro Dos Santos, Lin Wang, Derek A. T. Cummings,
Andrew S. Azman, Juliette Paireau, Arnaud Fontanet, Simon Cauchemez & Henrik Salje

This is a PDF file of a peer-reviewed paper that has been accepted for publication.
Although unedited, the content has been subjected to preliminary formatting. Nature
is providing this early version of the typeset paper as a service to our authors and
readers. The text and figures will undergo copyediting and a proof review before the
paper is published in its final form. Please note that during the production process
errors may be discovered which could affect the content, and all legal disclaimers
apply.

Article

Age-specific mortality and immunity patterns of SARS-CoV-2

<https://doi.org/10.1038/s41586-020-2918-0>

Received: 24 August 2020

Accepted: 23 October 2020

Published online: 2 November 2020

Megan O'Driscoll^{1,2}✉, Gabriel Ribeiro Dos Santos^{1,2}, Lin Wang^{1,2}, Derek A. T. Cummings³, Andrew S. Azman^{4,5}, Juliette Paireau^{2,6}, Arnaud Fontanet^{6,7}, Simon Cauchemez^{2,8}✉ & Henrik Salje^{1,2,8}✉

Estimating the size and infection severity of the SARS-CoV-2 epidemic is made challenging by inconsistencies in available data. The number of COVID-19 deaths is often used as a key indicator for the epidemic size, but observed deaths represent only a minority of all infections^{1,2}. Additionally, the heterogeneous burden in nursing homes and variable reporting of deaths in elderly individuals can hamper direct comparisons across countries of the underlying level of transmission and mortality rates³. Here we use age-specific COVID-19 death data from 45 countries and the results of 22 seroprevalence studies to investigate the consistency of infection and fatality patterns across multiple countries. We find that the age distribution of deaths in younger age groups (<65 years) is very consistent across different settings and demonstrate how this data can provide robust estimates of the share of the population that has been infected. We estimate that the infection-to-fatality ratio (IFR) is lowest among 5–9 years old, with a log-linear increase by age among individuals older than 30 years. Population age-structures and heterogeneous burdens in nursing homes explain some but not all of the heterogeneity between countries in infection-fatality ratios. Among the 45 countries included in our analysis, we estimate approximately 5% of these populations had been infected by the 1st of September 2020, with much higher transmission likely to have occurred in a number of Latin American countries. This simple modelling framework can help countries assess the progression of the pandemic and can be applied wherever reliable age-specific death data exists.

As SARS-CoV-2 continues its rapid global spread, increased understanding of the underlying level of transmission and infection severity are crucial for guiding pandemic response. While the testing of COVID-19 cases is a vital public health tool, variability in surveillance capacities, case-definitions and health-seeking behaviour can cause difficulties in the interpretation of case data. Due to more complete reporting, COVID-19 deaths are often seen as a more reliable indicator of epidemic size. If reliably reported, the number of COVID-19 deaths can be used to infer the total number of SARS-CoV-2 infections using estimates of the infection fatality ratio (IFR, the ratio of COVID-19 deaths to total SARS-CoV-2 infections). Estimates of the IFR derived from seroprevalence studies that carefully estimate the number of individuals with detectable antibodies can help make the link between deaths and total infections as well as refine estimates of the relative burden in different age groups¹. While it is clear that infection severity increases significantly with age^{2,4}, there remain key unanswered questions as to the consistency of mortality patterns across countries. Underlying heterogeneities in the age structure of the population, or in the prevalence of comorbidities can contribute to differences in the levels of observed COVID-19 fatalities⁵. In addition, when looking at the total number of

COVID-19 deaths, the level of transmission amongst the general population can be difficult to disentangle from large outbreaks in vulnerable populations such as nursing homes and other long-term care settings. Indeed for many countries, the SARS-CoV-2 pandemic has been characterized by a heavy burden in nursing home residents, with over 20% of all reported COVID-19 deaths occurring in nursing homes in countries such as Canada, Sweden and the United Kingdom⁶. In other countries, such as South Korea and Singapore, few COVID-19 deaths have been reported in nursing homes⁶. In this context, simply comparing the total number of deaths across countries may provide a misleading representation of the underlying level of transmission. Focusing on COVID-19 death data in younger individuals, however, may provide more reliable insights into the underlying nature of transmission.

Seroprevalence surveys provide valuable information on the proportion of the population that have ever experienced an infection^{7–10}, however, they can be subject to a number of biases and variable performance of different assays can complicate comparisons of results across studies¹¹. Here, we present a model framework that integrates age-specific COVID-19 death data from 45 countries with 22 national-level seroprevalence surveys, providing new insights into the

¹Department of Genetics, University of Cambridge, Cambridge, UK. ²Mathematical Modelling of Infectious Diseases Unit, Institut Pasteur, UMR2000, CNRS, Paris, France. ³Department of Biology and Emerging Pathogens Institute, University of Florida, Florida, USA. ⁴Department of Epidemiology, Johns Hopkins Bloomberg School of Public Health, Baltimore, USA. ⁵Unit of Population Epidemiology, Division of Primary Care Medicine, Geneva University Hospitals, Geneva, Switzerland. ⁶Emerging Infectious Diseases Unit, Institut Pasteur, Paris, France. ⁷PACRI unit, Conservatoire National des Arts et Métiers, Paris, France. ⁸These authors contributed equally: Simon Cauchemez, Henrik Salje. ✉e-mail: mo487@cam.ac.uk; simon.cauchemez@pasteur.fr; hs743@cam.ac.uk

consistency of infection fatality patterns across countries (Figure 1a). We use our model to produce ensemble IFR estimates by age and sex in a single harmonized framework as well as estimates of the proportion of the population infected in each country.

Age-specific mortality patterns

Using population age structures and age-specific death data, we compare the relative number of deaths by age within each country, using 55–59 year olds as the reference group. We find a very consistent pattern in the relative risk of death by age for individuals <65 years old across countries and continents, with a strong log-linear relationship between age and risk of death for individuals 30–65 years old (Figure 1b, Supplementary Methods S1). The observed relative risk of death in older individuals appears substantially more heterogeneous across locations. Given the potential for important variability in mortality associated with nursing home outbreaks across countries, we first investigate mortality patterns specifically in the general population, using age-specific deaths ≥65 from England, where granularity of the data allows us to remove deaths in nursing home populations. We find that the log-linear relationship between age and risk of death continues into older age groups (Figure 1b). To assess the generalizability of data from England to other countries, we use these estimates to reconstruct the number of non-nursing home deaths in 13 other countries and find the predictions consistent with reported numbers of non-nursing home deaths (Figure 1c, Supplementary Methods S2).

In order to translate relative risks of death by age to underlying IFR, we combine age-specific death data with 22 seroprevalence surveys, representing 16 of the 45 countries (multiple studies are available for Belgium, England, Scotland, Sweden and the Netherlands, Supplementary Table S1). We use daily time-series of reported deaths to reconstruct the timing of infections and subsequent seroconversions. To limit biases that can be introduced by outbreaks in nursing homes and potentially variable reporting practices of fatalities amongst individuals ≥65, we fit our model investigating the relationship between seroconversion and mortality exclusively to death data from those <65 years old. To infer IFRs in age groups ≥65 years, we use our estimates of the relative risk of death derived from England non-nursing home deaths. As our baseline model, we use an ensemble model where we include results from all national-level seroprevalence studies within a single framework. In addition, we consider separate models where we use the results of each individual serostudy to investigate the consistency of estimates provided by different studies. As older individuals have fewer social contacts¹² and are more likely to be isolated through shielding programmes we assume a baseline relative infection attack rate of 0.7 for individuals aged ≥65, relative to those <65, and assume equal infection attack rates across age groups <65 years. We find that age-specific IFRs estimated by the ensemble model range from 0.001% (95% Credible Interval [CrI]: 0–0.001) in those aged 5–9 (ranging from 0–0.002% across individual national-level serostudies) to 8.29% (95%CrI: 7.11–9.59%) in those aged 80+ (range: 2.49–15.55% across individual national-level serostudies) (Figure 2a). We estimate a mean increase in IFR of 0.59% with each 5-year increase in age (95%CrI: 0.51–0.68%) for ages ≥10. We estimate that the risk of death given infection for men is significantly higher than that of women (Figure 2a) particularly in older individuals with ensemble IFR estimates of 10.83% for men aged 80+ (95%CrI: 9.28–12.52%, individual serostudy range: 3.25–20.30%) and 5.76% for women aged 80+ (95%CrI: 4.94–6.66%, individual serostudy range: 1.73–10.80%), consistent with previous findings^{13,14}.

Consistency of IFRs across serostudies

We use our model framework to facilitate robust comparisons of IFRs across settings, considering only age-specific deaths amongst <65 year olds. Using country-specific demographic distributions (both age and

sex) we estimate population-weighted IFRs for each country. Taking France as a reference population, the ensemble model estimates a population IFR of 0.79% (95%CrI: 0.68–0.92%) though we find notable heterogeneity in IFR estimates as suggested by individual national-level seroprevalence studies, with a median range of 0.24–1.49% (Figure 2b). In particular, seroprevalence studies from New York City (2.28, 95%CrI: 2.15–2.42%), Scotland (1.49%, 95%CrI: 1.25–1.82%) and England (1.41%, 95%CrI: 1.38–1.44%) suggest a significantly higher IFR while studies in Kenya (0.24%, 95%CrI: 0.23–0.25%), Slovenia (0.25%, 95%CrI: 0.24–0.30%) and Denmark (0.26%, 95%CrI: 0.24–0.32%) support a lower IFR than that of the ensemble model. We note that, the application of age- and sex-specific IFR estimates suggested by individual national-level seroprevalence studies at the lower end of the scale (e.g. Kenya, Slovenia, Denmark), to mortality data in highly-impacted settings would imply attack rates >100% (Figure S3). Potential explanations for the variable IFR estimates observed across settings include different prevalences of high-risk populations (e.g. individuals with comorbidities), differences in methodology and representativeness of seroprevalence studies, heterogeneities in availability and quality of care or variations in reporting of COVID-19 deaths. We have fit our model to seroprevalence data adjusted for reported assay sensitivity and specificity but find that using unadjusted estimates provides similar results (Figure S5). As the duration of SARS-CoV-2 seropositivity amongst infected individuals is as-yet unclear¹⁵, in sensitivity analyses we explore the potential effect of waning antibodies over time. In an extreme scenario with assumed 5% exponential decay of seroconversions per month the ensemble model estimates a population IFR of 0.65% in France (95%CrI: 0.56–0.73%) (Figure S4). Further, we demonstrate that our results are robust to different assumptions regarding the mean delay between infection and seroconversion (Figure S4). There may also be individuals who never seroconvert or only develop a T-cell response, and would be missed in these studies¹⁶. Of the studies included in our analysis, we find that those conducted amongst blood donors (which exclude children and require individuals to be asymptomatic at the time of sampling) do not give significantly different results to those conducted amongst the general population (Figure S6). However, further comparisons are needed to fully understand the representativeness of different serological study designs.

Considering the demographic structures of each country, we find that population-weighted IFR estimates by the ensemble model are highest for countries with older populations such as Japan (1.09%, 95%CrI: 0.94–1.26%, individual serostudy range: 0.33–2.05%) and Italy (0.94%, 95%CrI: 0.80–1.08%, individual serostudy range: 0.28–1.76%), whilst the lowest IFRs are for Kenya (0.09%, 95%CrI: 0.08–0.10%, individual serostudy range: 0.03–0.17%) and Pakistan (0.16%, 95%CrI: 0.14–0.19%, individual serostudy range: 0.05–0.31%) (Figure 2c). Our ensemble model reproduces the reported seroprevalence values for the majority of studies including temporal dynamics. However, consistent with a substantial heterogeneity in IFR across countries, the ensemble model cannot fully reconcile the relationship between reported seroprevalence and age-specific death data in some locations (Figure 3b). Of the 45 countries included in our analysis, representing 3.4 billion people, we estimate an average of 5.27% (95%CrI: 4.51–6.20%, individual serostudy range: 2.80–13.97%) of these populations had been infected by the 1st of September 2020 ranging from 0.06% (95%CrI: 0.04–0.09%, individual serostudy range: 0.02–0.20%) in South Korea to 62.44% (95%CrI: 54.07–72.90%, individual serostudy range: 33.13–207.20%) in Peru. These results indicate large heterogeneity in the level of transmission across countries, with particularly high attack rates estimated in many South American countries. Given the underlying heterogeneity in IFR that could not be captured by the ensemble model, it is important to consider the full range of uncertainty in these estimates as suggested by individual seroprevalence studies (grey points in Figure 3b). Estimates of high transmission levels in some South American countries are consistent with recent subnational seroprevalence studies^{17–19}. Our

estimates are also consistent with mathematical modelling efforts for individual countries, where additional metrics of epidemic size (e.g. numbers of cases, hospitalizations and/or ICU admissions) have been considered^{13,20,21} (Figure S7). The medium and longer term implications for the pandemic in countries which have experienced high levels of infection remain unclear; in particular, whether there exists sufficient immunity to halt the epidemic locally²².

Heterogeneities in ≥ 65 mortality

Using our model framework we estimate the number of deaths expected in the absence of nursing home transmission in those aged ≥ 65 years, given the reported number of deaths in younger age groups, and compare them to the reported number of COVID-19 deaths in ≥ 65 year olds (Figure 4a). We find that many countries in South America had significantly fewer reported deaths in individuals ≥ 65 years than expected, consistent with under-reporting of COVID-19 deaths amongst elderly individuals. For example, we find that in Ecuador there are 220 fewer reported deaths per 100,000 in those ≥ 65 years than expected (95%CrI: 200–240), equivalent to approximately 2,800 missing deaths. While lower infection attack rates in elderly populations due to reduced contacts or successful shielding policies may also explain lower mortality rates, in sensitivity analyses we show that for some countries unrealistically low infection attack rates amongst ≥ 65 year olds compared to the rest of the population would be required to reconcile the reported number of deaths in these age-groups (Figure S8).

By contrast, for many European countries we observe a higher incidence of deaths in older individuals than expected (Figure 4a). This is consistent with the large proportion of reported COVID-19 deaths attributable to outbreaks in nursing homes, highlighting the enormous burden experienced by these communities in many higher-income countries^{23,24}. We use the age and sex-distribution of nursing home residents to derive a population-weighted IFR of 22.25% (95%CrI: 19.06–25.74%) among French nursing home residents, assuming individuals in nursing homes are 3.8 times more frail than individuals in the general population of the same age and sex, as previously estimated²⁵ (Figure 4b). Using this estimate of the IFR would suggest that 7.28% of the French nursing home population had been infected by the 1st of September 2020 (95%CrI: 6.29–8.49%), a 1.70 fold higher infection attack rate than the general population (Supplementary Methods S3). In our baseline model we derive IFR estimates amongst the general population (i.e. excluding nursing home deaths) so as to facilitate robust comparisons of IFR and general population transmission across settings. However, we demonstrate that where high rates of infection have occurred amongst nursing home residents, overall IFRs will be significantly greater than in scenarios where these populations have been successfully shielded or experienced little exposure (Figure 4c). For example, in France, including nursing homes deaths increases the IFR from 0.74% for the general population (95%CrI: 0.64–0.86%) to 1.10% overall (95%CrI: 0.95–1.28%). This highlights the complexity in comparing headline IFR estimates across populations where very different levels of transmission may have occurred in these hyper-vulnerable communities.

Discussion

In our analysis we assess the relationship between seroprevalence and the age-specific number of COVID-19 deaths across many settings. Accounting for population demographics and variable mortality burdens amongst elderly populations, we find considerable heterogeneity in the overall IFR of SARS-CoV-2 across settings, suggesting additional important drivers of infection fatality ratios.

Seroprevalence surveys have, to date, shown inconsistent patterns in age-specific infection attack rates across settings (Figure S10) as contact patterns are likely to have changed significantly over the course

of the pandemic. In sensitivity analyses we find our results to be relatively consistent when using different assumed age-specific infection attack rates (Figure S9). Here we have used data from national reporting systems of COVID-19 associated deaths. However, in some settings these may not capture all deaths associated with COVID-19. It has been estimated for a subset of countries ($N=6/45$) that reported COVID-19 deaths were between 40% undercounted to 10% overcounted as compared to excess death estimates²⁶. Assuming that these differences occur equally across all age groups would result in a change of mean IFR for these countries of 0.66% to 0.87%. Note that this represents an extreme scenario, as most unaccounted for deaths are likely to be in the oldest age groups, which would not affect our estimates²⁶. We note that there are a number of complexities in the interpretation of excess death data that can inhibit their direct use in assessments of IFR. Specifically, excess death estimates are highly sensitive to the reference time period used (Figures S11–S12), frequent negative excess deaths occur, especially in younger ages (Figure S12), and there is limited availability of excess deaths for narrow age-groups or outside resource-rich countries. While both seroprevalence and reported COVID-19 death data can be subject to potential limitations, considering these data across multiple settings in a harmonized framework allows us to robustly assess trends in the transmission and fatality rates of SARS-CoV-2 and derive global ensemble estimates.

Translating the number of COVID-19 deaths into estimates of the number of infections requires careful consideration of fatalities from outbreak events in highly vulnerable populations. By providing a benchmark of the expected number of deaths by age in older individuals, our approach allows us to identify countries where excess transmission in nursing home populations has likely occurred. We demonstrate how outbreaks in nursing homes can drive overall population IFRs, through both increased attack rates and increased vulnerability. The results and modelling framework we present demonstrate how age-specific death data can be used to robustly reconstruct the underlying level of transmission. This approach could be applied at sub-national scale and may be of particular use in settings where there do not exist the resources to carry out large, representative seroprevalence studies.

Online content

Any methods, additional references, Nature Research reporting summaries, source data, extended data, supplementary information, acknowledgements, peer review information; details of author contributions and competing interests; and statements of data and code availability are available at <https://doi.org/10.1038/s41586-020-2918-0>.

- Pastor-Barriuso, R. et al. SARS-CoV-2 infection fatality risk in a nationwide seroepidemiological study. *medRxiv* (2020).
- Verity, R. et al. Estimates of the severity of coronavirus disease 2019: a model-based analysis. *Lancet Infect. Dis.* **20**, 669–677 (2020).
- Comas-Herrera, A., Zalakain, J., Litwin, C., T Hsu, A. & Fernandez-Plotka, J.-L. Resources to support community and institutional Long-Term Care responses to COVID-19. (2020).
- Guan, W.-J. et al. Clinical Characteristics of Coronavirus Disease 2019 in China. *N. Engl. J. Med.* **382**, 1708–1720 (2020).
- Clark, A. et al. Global, regional, and national estimates of the population at increased risk of severe COVID-19 due to underlying health conditions in 2020: a modelling study. *Lancet Glob Health* **8**, e1003–e1017 (2020).
- Comas-Herrera, A. et al. Mortality associated with COVID-19 outbreaks in care homes: early international evidence. *LTCcovid. org, International Long-Term Care Policy Network* (2020).
- Pollán, M. et al. Prevalence of SARS-CoV-2 in Spain (ENE-COVID): a nationwide, population-based seroepidemiological study. *Lancet* (2020) [https://doi.org/10.1016/S0140-6736\(20\)31483-5](https://doi.org/10.1016/S0140-6736(20)31483-5).
- Stringhini, S. et al. Seroprevalence of anti-SARS-CoV-2 IgG antibodies in Geneva, Switzerland (SEROCOV-POP): a population-based study. *Lancet* **396**, 313–319 (2020).
- Rosenberg, E. S. et al. Cumulative incidence and diagnosis of SARS-CoV-2 infection in New York. *Ann. Epidemiol.* **48**, 23–29.e4 (2020).
- Herzog, S. et al. Seroprevalence of IgG antibodies against SARS coronavirus 2 in Belgium: a prospective cross-sectional study of residual samples. *medRxiv* (2020).
- Takahashi, S., Greenhouse, B. & Rodríguez-Barraquer, I. Are SARS-CoV-2 seroprevalence estimates biased? (2020).

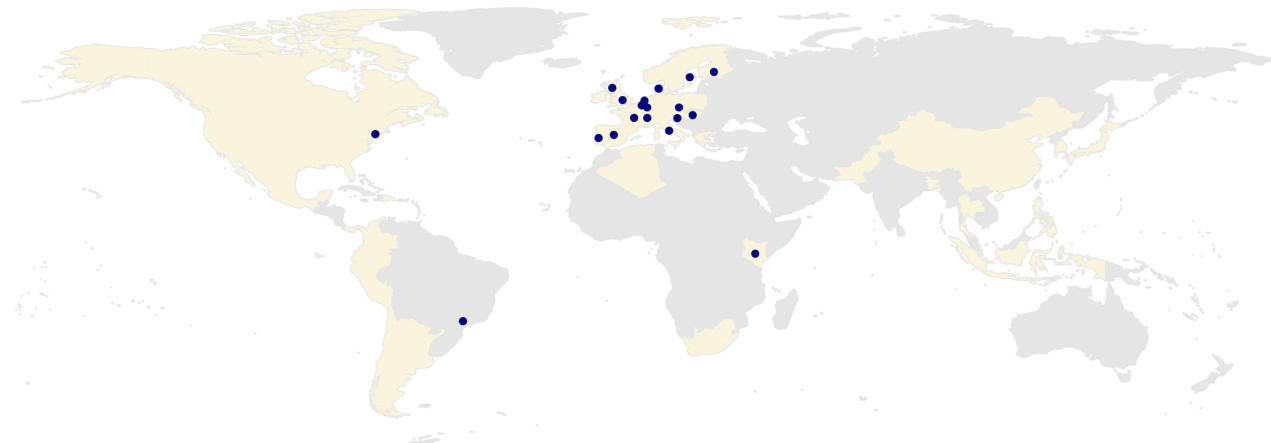
- ACCELERATED ARTICLE PREVIEW
-
12. Prem, K., Cook, A. R. & Jit, M. Projecting social contact matrices in 152 countries using contact surveys and demographic data. *PLoS Comput. Biol.* **13**, e1005697 (2017).
 13. Salje, H. et al. Estimating the burden of SARS-CoV-2 in France. *Science* **369**, 208–211 (2020).
 14. Jin, J.-M. et al. Gender Differences in Patients With COVID-19: Focus on Severity and Mortality. *Front Public Health* **8**, 152 (2020).
 15. Huang, A. T. et al. A systematic review of antibody mediated immunity to coronaviruses: kinetics, correlates of protection, and association with severity. *Nat. Commun.* **11**, 4704 (2020).
 16. Braun, J. et al. SARS-CoV-2-reactive T cells in healthy donors and patients with COVID-19. *Nature* (2020) <https://doi.org/10.1038/s41586-020-2598-9>.
 17. Buss, L. F. et al. COVID-19 herd immunity in the Brazilian Amazon. *medRxiv* (2020).
 18. Antonio, C. A. A. et al. Seroprevalencia de anticuerpos anti SARS-CoV-2 en la ciudad de Iquitos, Loreto, Perú. <https://docs.google.com/document/d/1K-aKyFmxztdfNjOtXuSH1uGcBeaZA7LH/edit>.
 19. Del Brutto, O. H. et al. SARS-CoV-2 in rural Latin America. A population-based study in coastal Ecuador. *Clin. Infect. Dis.* (2020) <https://doi.org/10.1093/cid/ciaa1055>.
 20. Flaxman, S. et al. Estimating the effects of non-pharmaceutical interventions on COVID-19 in Europe. *Nature* (2020) <https://doi.org/10.1038/s41586-020-2405-7>.
 21. Abrams, S. et al. Modeling the early phase of the Belgian COVID-19 epidemic using a stochastic compartmental model and studying its implied future trajectories. *medRxiv* (2020).
 22. Fontanet, A. & Cauchemez, S. COVID-19 herd immunity: where are we? *Nat. Rev. Immunol.* **20**, 583–584 (2020).
 23. Molenberghs, G. et al. Belgian Covid-19 Mortality, Excess Deaths, Number of Deaths per Million, and Infection Fatality Rates (8 March - 9 May 2020). <https://doi.org/10.1101/2020.06.20.20136234>.
 24. Soveri, H. et al. Why, in almost all countries, was residential care for older people so badly affected by COVID-19?
 25. Hardy, O. J. et al. A world apart: levels and factors of excess mortality due to COVID-19 in care homes. The case of Wallonia-Belgium. *medRxiv* (2020).
 26. Aron, J., Giattino, C., Muellbauer, J. & Ritchie, H. A pandemic primer on excess mortality statistics and their comparability across countries. Accessed August **19**, 2020 (2020).

Publisher's note Springer Nature remains neutral with regard to jurisdictional claims in published maps and institutional affiliations.

© The Author(s), under exclusive licence to Springer Nature Limited 2020

Article

A



B

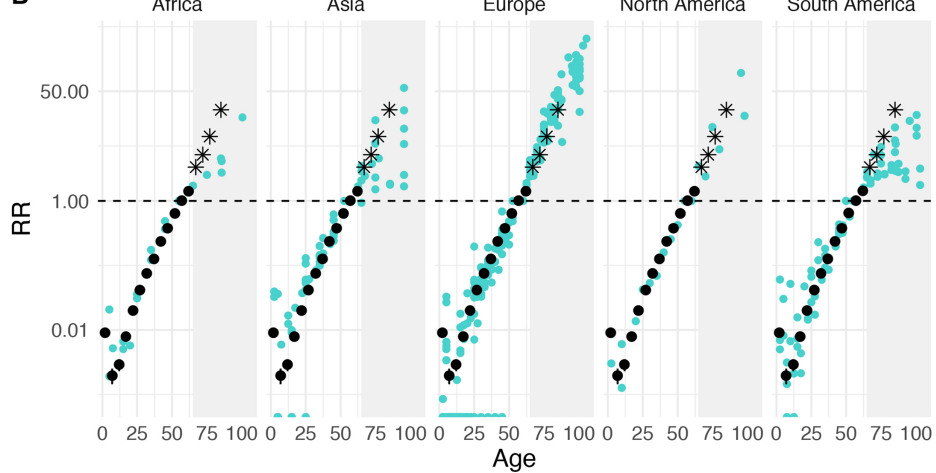
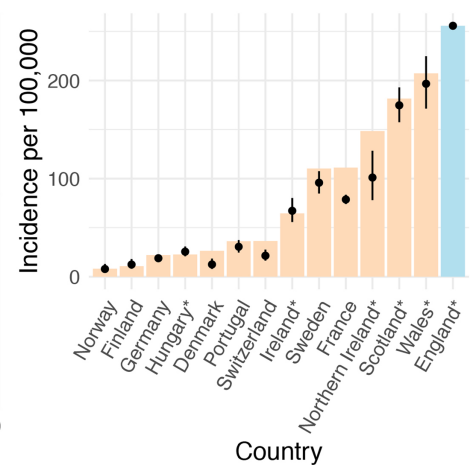


Fig. 1 | Patterns of COVID-19 mortality across settings. (A) Countries with age-specific death data (beige tiles) and locations with seroprevalence data (coloured points). (B) Estimated median and 95% credible interval (Crl) of the proportion of the population that have died in each age group, relative to the proportion that have died among 55–59 year olds in that country (black dots and lines), plotted on a log-linear scale. Coloured dots represent the country- and age-specific risks of COVID-19 death in the population relative to that of 55–59 year olds observed from reported death data, accounting for population age distributions (Supplementary Methods S1) ($N=538,477$ reported deaths). All data points are plotted at the midpoint of the reported age group. The grey

C Reconstructed deaths >60



shaded areas highlight the relative risks of death by age for age groups ≥ 65 , excluded from model fitting and black stars represent estimates inferred from England data only which are derived independent of nursing home deaths. (C) Comparing the reconstructed number of deaths with reported data for age-groups 60 or 65+ for a subset of countries where nursing home deaths could be excluded. Black dots and lines indicate the estimated median and 95% Crl; coloured bars show the reported incidence of non-nursing home deaths aged ≥ 60 . Countries labelled with an asterisk * indicate where the number of deaths were reconstructed for ages 65+, to align with the reported age-groups for each country.

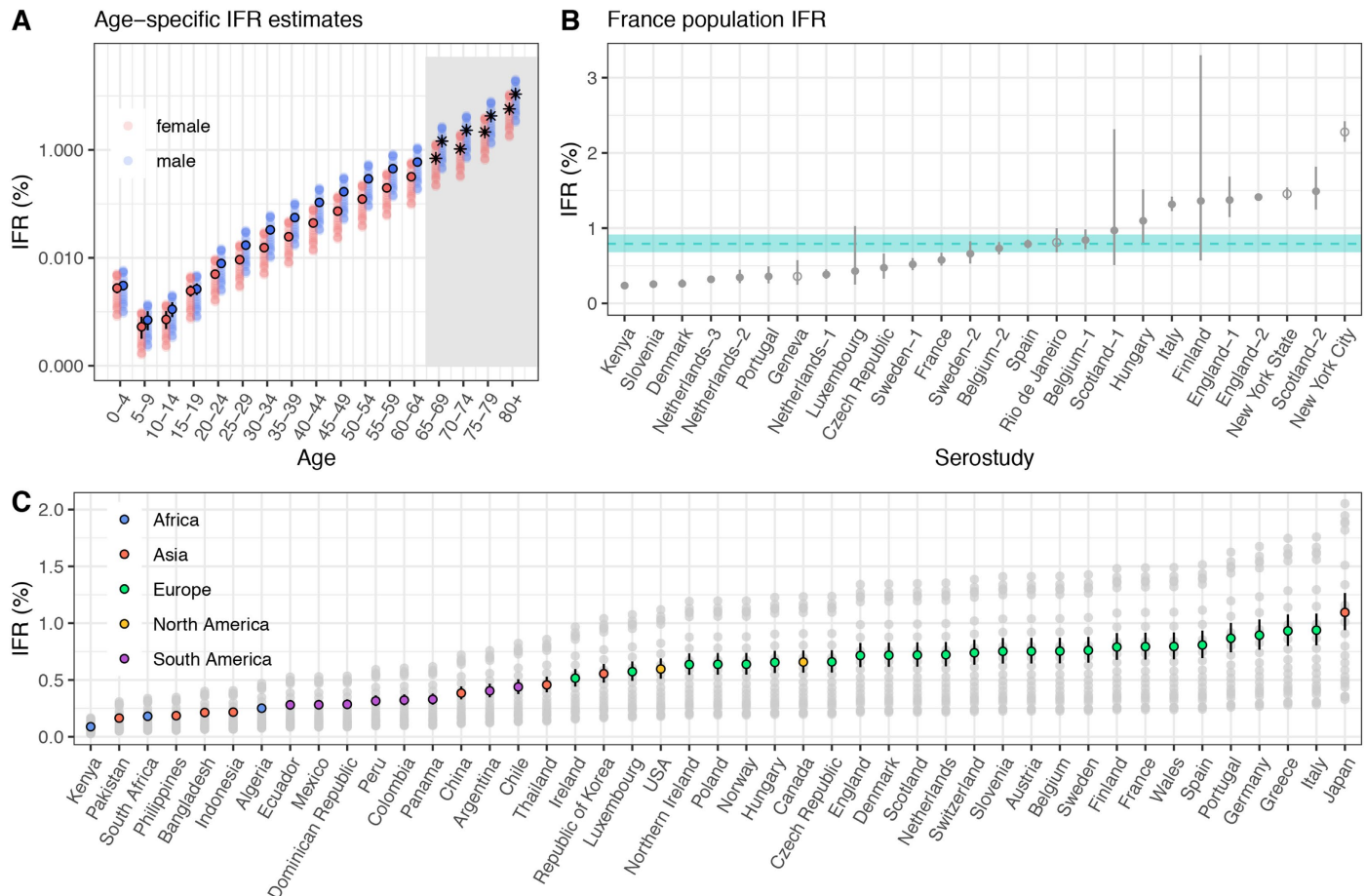


Fig. 2 | Infection fatality ratio (IFR) estimates. (A) Estimated median and 95% credible interval (CrI) of the IFR, stratified by age and sex and plotted on a log-linear scale. The IFR is estimated with the ensemble model (filled dots and black lines). Black stars on the right-hand side represent the estimated IFRs for age-groups ≥ 65 , which were excluded from the fitting of the ensemble model. The coloured shaded dots represent median IFRs estimated from separately fitting to each individual serosurvey. (B) Population-weighted IFR estimates derived from separately fitting individual serological surveys in the model and using France as a reference population, with points and lines indicating the

median and 95%CrI. The blue dashed line and ribbon indicate the median and 95%CrI of the population-weighted IFR produced by the ensemble model. Hollow dots represent the estimates from subnational serological surveys that were excluded from the fitting of the ensemble model. (C) Median and 95%CrI of the population-weighted IFRs estimated by the ensemble model for each of the 45 countries, coloured by continent. Grey shaded dots represent the median estimates for each country, derived from fitting the model separately to each individual seroprevalence survey.

Article

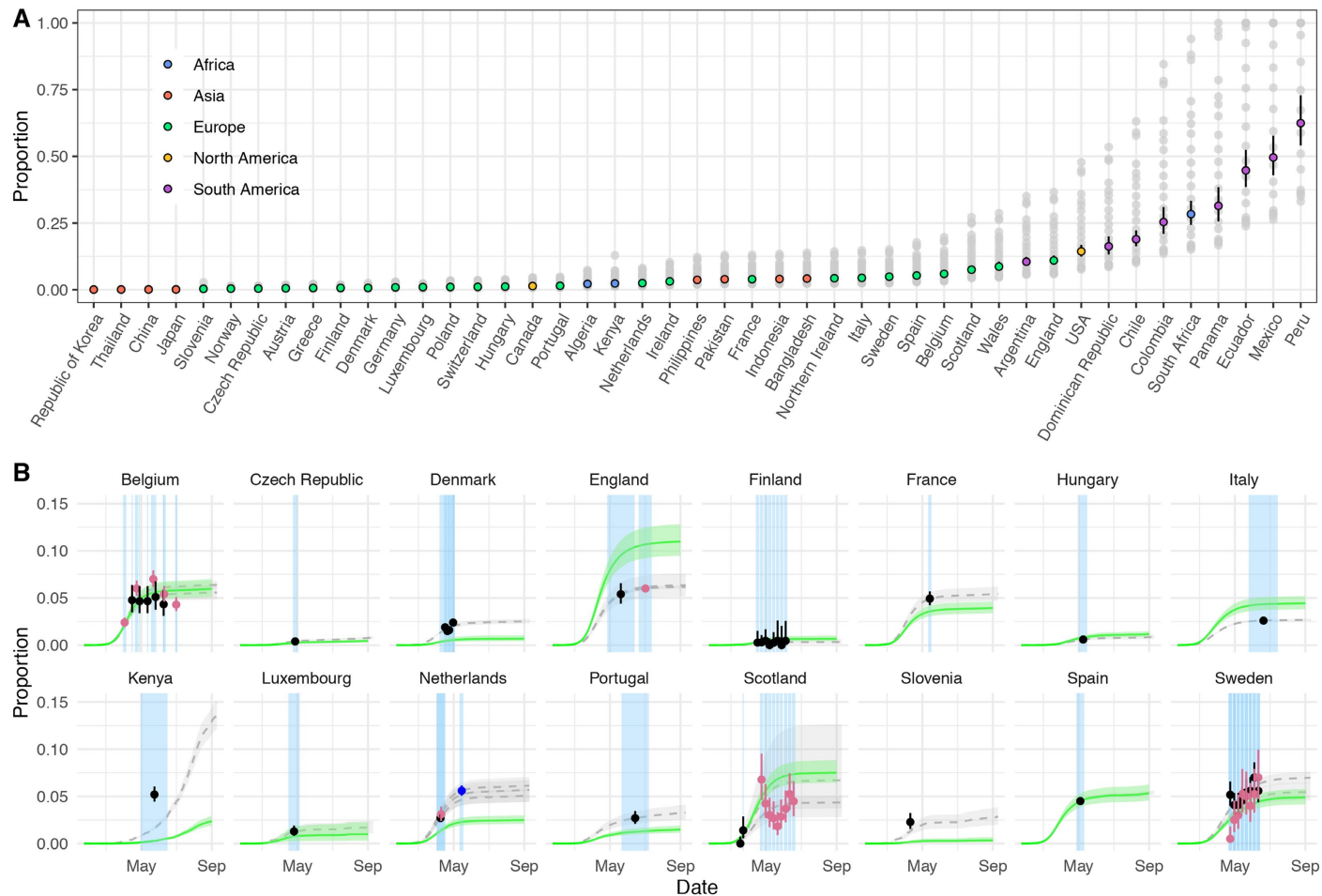


Fig. 3 | Infection attack rates. (A) Estimates of the infected population proportion for each country as of the 1st of September 2020*. Grey shaded dots indicate the median estimates by fitting the model with each individual seroprevalence survey. Coloured dots and lines represent the median and 95% credible intervals (Crl) estimated by the ensemble model. *The y-axis has been capped at 1. In Figure S4 we show the same graph with the full range of values. (B) Proportion seropositive over time for each of the 12 countries with national-level seroprevalence data. Green curve and ribbon indicate the median and 95% Crls estimated by the ensemble model. Dots and lines

represent the mean and 95% binomial confidence interval reported by the published seroprevalence data. For countries with >1 seroprevalence surveys, black dots and lines correspond to the study-1 as referenced in Figure 2 and Supplementary Table S1, whereas pink dots and lines correspond to the study-2 (e.g. Belgium-2) and navy dots and lines to study-3. Blue shaded regions indicate the start and end dates of sampling for each seroprevalence survey. Grey dashed lines and ribbons represent the median and 95% Crl model estimates derived from separately fitting to each individual serostudy.

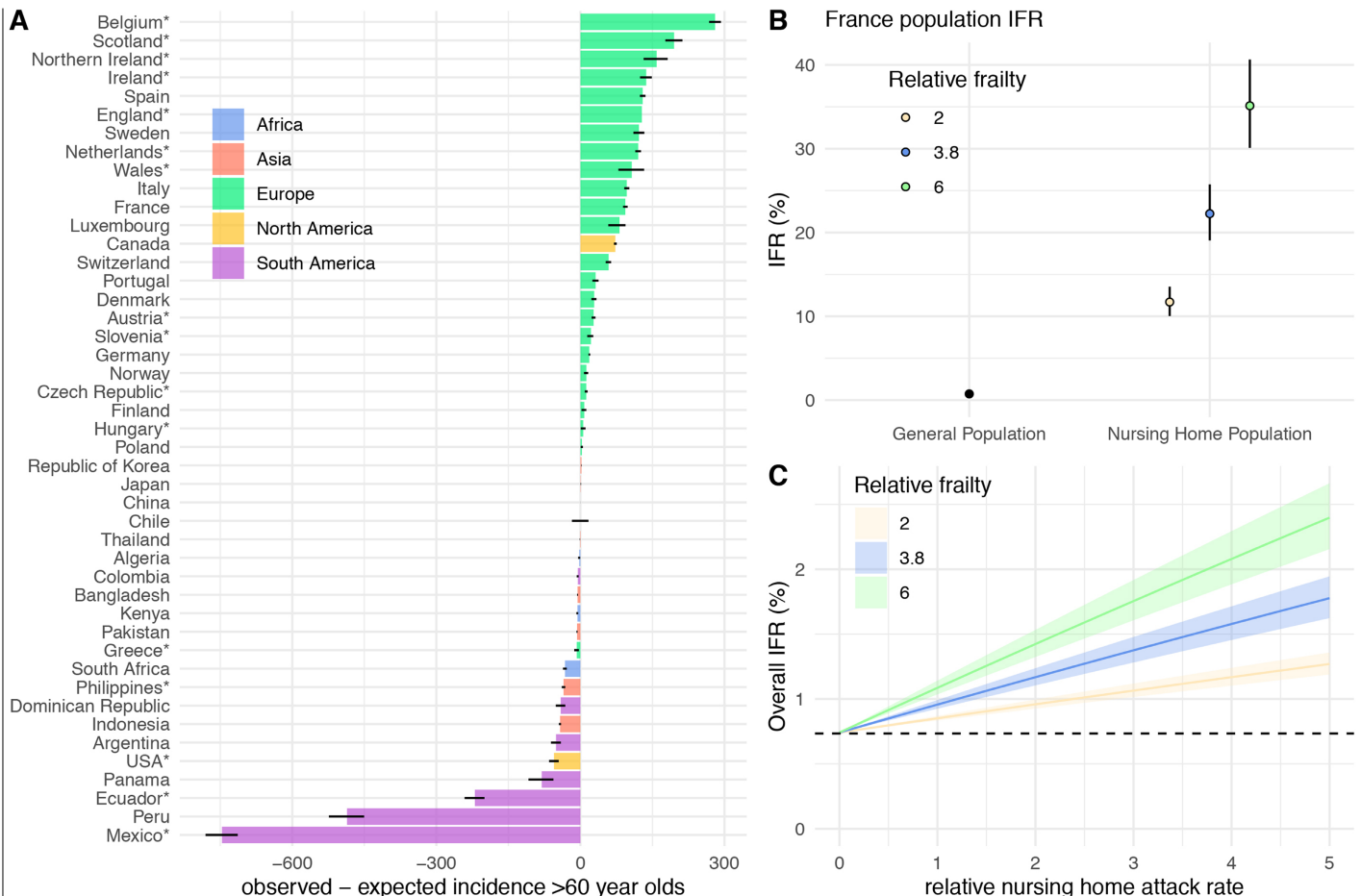


Fig. 4 | Infection fatality patterns amongst ≥ 60 s. (A) Difference between the reported and expected incidence of COVID-19 deaths per 100,000 population amongst ≥ 60 s or ≥ 65 s in each country. Coloured bars represent the median difference and black lines represent 95% credible intervals (Crls). Countries labelled with an asterisk * indicate where the number of deaths were reconstructed for ages 65+, to align with the reported age-groups for each country ($N=429,039$ reported deaths 60 or 65+). (B) Population-weighted IFRs for the general population and nursing home residents, using France as a reference population ($N=10,560$ reported deaths amongst nursing home residents and $N=20,528$ amongst the general population). The relative frailty of

nursing home residents is assumed to be 2 (yellow), 3.8 (green), or 6 (blue). Dots and lines indicate the median and 95% Crls estimated by the ensemble model. (C) Population-weighted IFR in France, estimated with different assumed infection attack rates and frailty of nursing home residents relative to those of the same age and sex in the general population. Coloured ribbons indicate 95% Crls and the black dashed line represents the median population-weighted IFR estimated when assuming a zero infection attack rate amongst nursing home residents ($N=10,560$ reported deaths amongst nursing home residents and $N=20,528$ amongst the general population).

Article

Methods

Data

Age- and sex- specific COVID-19 fatality data. We collated national-level age-stratified COVID-19 death counts from official government and department of health webpages and reports for 45 countries. Where available, the stratification by both age and sex were used. Sub-national age-stratified death counts were additionally collated for 4 regions where seroprevalence surveys had been conducted. For countries where information on age was missing for a subset of deaths, we assumed the age-distribution of the missing subset to be the same as that of the deaths with available age data. Information on age was missing for 29% of deaths in Spain. In addition, the time series of daily reported deaths from each country/region were obtained from the COVID-19 Data Repository by the Center for Systems Science and Engineering (CSSE) at Johns Hopkins University²⁷. Age- and sex-specific population data were obtained from the United Nations 2019 World Population Prospects^{28,29}.

Seroprevalence studies. We used data from 25 SARS-CoV-2 seroprevalence surveys from 20 countries/regions where the results were representative of the general population and where age-stratified death data were also available, shown in Figure 1a and Supplementary Table S1. In the ensemble model we consider only the 22 national-level seroprevalence surveys, representing 16 countries. Where estimates of seroprevalence reported by individual studies had not been adjusted for the performance of the serological assay, we used the reported values of assay sensitivity and specificity to adjust the reported values (Supplementary Table S1). Seroprevalence values from 24/25 studies included in our analysis were adjusted for assay performance, while the serological assay used by the remaining 1 study had not been reported at the time of publishing.

Model

We combined age- and sex-specific COVID-19 death data from 45 countries with data from 15 seroprevalence surveys, to jointly infer the age- and sex-specific IFRs and country-specific cumulative probabilities of infection. Age- and sex-specific IFRs were estimated in 5-year age-groups, with individuals aged 80+ considered as a single age group. Let $N_{c,a,s}$ be the population size for the age group a of sex s in country c . The expected number of deaths for the age group a of sex s in country c , $D_{c,a,s}$ is estimated as shown in equation 1, which we assume to follow a Poisson distribution. Λ_c denotes the cumulative probability of infection in country c , δ_a the relative probability of infection in age-group a , and $IFR_{a,s}$ the infection fatality ratio of age-group a and sex s . This assumes that age- and sex-specific IFRs are constant over the course of the pandemic. Where improvements in COVID-19 outcomes have occurred over time, our estimates would represent the average probabilities to-date.

$$D_{c,a,s} = N_{c,a,s} \cdot \Lambda_c \cdot \delta_a \cdot IFR_{a,s} \quad (1)$$

The expected number of deaths estimated by 5-year age-groups were summed to match the corresponding age-groups of observed deaths when reported in coarser age-groups. We fit exclusively to the reported number of deaths for age groups <65 years for each country (i.e. including all age-groups where the upper bound is <65 years). IFRs for age groups ≥65 were derived from age-specific death data reported by the Office for National Statistics (ONS) in England³⁰, which allows us to exclude the age-specific number of deaths among nursing home residents (Supplementary Methods S2). As an external validation, we apply these IFRs to reported death data for a subset of 13 countries where an adjustment for deaths occurring in nursing homes could be applied (Supplementary Methods S2).

To align estimates of the cumulative probability of infection, Λ_c , with data from seroprevalence surveys, we used daily time-series of

reported deaths to infer the timing of infections and subsequent seroconversions. We assumed a gamma distributed delay between onset and death with mean of 20 and standard deviation of 10 days³¹ and a gamma distributed delay between infection and onset with mean 6.5 and standard deviation 2.6 days³². The delay between onset and seroconversion was assumed to be gamma distributed with a mean of 10 and standard deviation of 8 days³³. We derive the approximated seroprevalence at a given survey period t , $\lambda_{c,t}$, as shown in equation 2. Here, $S_{c,i}$ is the inferred number of seroconversions in country c on day i , as inferred from the convolution of the death time-series, $D_{c,i}$ is the number of new deaths reported in country c on day i , and T_c is the date of reporting of the age-stratified cumulative death data.

$$\lambda_{c,t} = \Lambda_c \cdot \sum_{i=1}^t S_{c,i} / \sum_{i=1}^{T_c} D_{c,i} \quad (2)$$

We include all data from national-level seroprevalence studies in an ensemble model, where the expected seroprevalence is assumed to follow a Beta distribution with unknown variance parameter, κ , as shown in equation 3. To investigate the contribution of different serological studies to the likelihood the model was fit separately to data from each individual seroprevalence survey, including an additional 3 subnational seroprevalence studies (Supplementary Table S1). For each seroprevalence survey the expected number of seropositive individuals in country c at sampling period t , $NPos_{c,t}$, is assumed to follow a Binomial distribution as shown in equation 4, where $NSamples_{c,t}$ is the number of serological samples taken in country c at time t ³⁴.

$$\bar{\lambda}_{c,t} \sim Beta(\lambda_{c,t}, \kappa) \quad (3)$$

$$NPos_{c,t} \sim Binomial(NSamples_{c,t}, \lambda_{c,t}) \quad (4)$$

All parameters were estimated in a Bayesian framework using RStan³⁵ using R version 3.6.1. We assumed uniform priors on all parameters, between -50 and -0.001 on a log scale for all IFR estimates, and between -50 and 2 on a log scale for all estimates of the cumulative probability of infection. The model was run with 3 chains of 10,000 iterations each. 95% credible intervals (CrI) are calculated by taking the 0.025 and 0.975 quantiles of the posterior distribution.

Reporting summary

Further information on research design is available in the Nature Research Reporting Summary linked to this paper.

Data Availability

Data is available at <https://github.com/meganodris/International-COVID-IFR>. Queries can be addressed to mo487@cam.ac.uk

Code Availability

All code necessary to reproduce this analysis is available at <https://github.com/meganodris/International-COVID-IFR>

27. Dong, E., Du, H. & Gardner, L. An interactive web-based dashboard to track COVID-19 in real time. *Lancet Infect. Dis.* **20**, 533–534 (2020).
28. De Wulf, M. Population Pyramids of the World from 1950 to 2100. (2016).
29. World Population Prospects - Population Division - United Nations. <https://population.un.org/wpp/>.
30. Caul, S. Deaths registered weekly in England and Wales, provisional. (2020).
31. Wu, J. T. et al. Estimating clinical severity of COVID-19 from the transmission dynamics in Wuhan, China. *Nat. Med.* **26**, 506–510 (2020).
32. Backer, J. A., Klinkenberg, D. & Wallinga, J. Incubation period of 2019 novel coronavirus (2019-nCoV) infections among travellers from Wuhan, China, 20–28 January 2020. *Euro Surveill.* **25**, (2020).

33. Lou, B. et al. Serology characteristics of SARS-CoV-2 infection since exposure and post symptom onset. *Eur. Respir. J.* (2020) <https://doi.org/10.1183/13993003.00763-2020>.
34. Wu, J. T. et al. The infection attack rate and severity of 2009 pandemic H1N1 influenza in Hong Kong. *Clin. Infect. Dis.* **51**, 1184–1191 (2010).
35. Stan Development Team. RStan: the R interface to Stan. *R package version 2*, (2016).

Acknowledgements We acknowledge financial support from the EPSRC Impact Acceleration Grant (number RG90413) (MO'D, HS, GRDS, LW), the European Research Council (grant 804744) (HS), the Investissement d'Avenir program (SC), the Laboratoire d'Excellence Integrative Biology of Emerging Infectious Diseases program (grant ANR-10-LABX-62-IBEID) (SC), Santé Publique France (SC), the INCEPTION project (PIA/ANR16-CONV-0005) (SC), and the European Union's Horizon 2020 research and innovation program under grants 101003589 (RECOVER) and 874735 (VEO) (SC). We thank the global public health community for the rapid synthesis of SARS-CoV-2 data.

Author contributions MO'D, HS and SC conceived the study and performed the analysis. MO'D, HS, SC, GRDS, LW, and JP collated data. GRDS and LW reviewed code. MO'D, HS and SC wrote the first draft of the manuscript. MO'D, HS, SC, GRDS, LW, DATC, ASA, JP and AF discussed the results and contributed to revisions of the manuscript.

Competing interests The authors declare no competing interests.

Additional information

Supplementary information is available for this paper at <https://doi.org/10.1038/s41586-020-2918-0>.

Correspondence and requests for materials should be addressed to M.O., S.C. or H.S.

Peer review information *Nature* thanks Gabriel Leung, Geert Molenberghs and the other, anonymous, reviewer(s) for their contribution to the peer review of this work. Peer reviewer reports are available.

Reprints and permissions information is available at <http://www.nature.com/reprints>.

ACCELERATED ARTICLE PREVIEW